Journal of Applied Polymer Science

Influence of the rubber content and particle morphology on the mechanical properties of the (hiPP)

Nabila Amiar,[1] Djallel Bouzid,[1,2] Timothy F.L McKenna[3]

[1]Materials Science and Technology Research Unit, Research Center of Industrial Technologies, Constantine 25000, Algeria
[2]National Polytechnic School of Constantine, Constantine 25000, Algeria
[3]Chemistry, Catalysis, Polymers & Processes C2P2-UCBL/CNRS/ESCPE-Lyon, Villeurbanne 69000, France
Correspondence to: D. Bouzid (E-mail: bouziddjallel@yahoo.fr)

ABSTRACT: The effect of the final morphology and the role of ethylene propylene rubber (EPR) content and (iPP) particle size on the mechanical properties of (iPP/EPR) *in situ* blends are investigated. The addition of EPR causes a significant improvement in the impact strength of the composites, from 20 kJ/m^2 in unthoughned composite iPP to 100 kJ/m^2 in iPP/EPR composites containing 50% EPR. Conversely, the tensile strength and the Young's modulus of the blends decrease as the EPR amount increases. The mechanical tensile strength is similar for the composite which have a time of homopolymerization less or equal to 60 min, and a higher value is observed in the case of 100 min. The scanning electron microscopy characterization shows that the larger the iPP particle is, the less the rubber settles on the surface of the high impact polypropylene and the less the final material is resistant to shocks. © 2016 Wiley Periodicals, Inc. J. Appl. Polym. Sci. **2016**, *133*, 44197.

KEYWORDS: ethylene-propylene rubber; hiPP mechanical properties; hiPP particle morphology

Received 22 May 2016; accepted 18 July 2016
DOI: 10.1002/app.44197

INTRODUCTION

The blending of two or more types of polymers is a useful technique for the preparation and development of materials with properties superior to those of the individual constituents.[1,2]

It is well known that the poor impact properties of isotactic polypropylene iPP can be improved by blending isotactic polypropylene with ethylene propylene rubber (EPR).[3,4] Recently, a novel copolymerization technology which produces an *in situ* polypropylene copolymer by a two-step polymerization has been widely applied in industry.[5,6]

In comparison to iPP/EPR blends formed by mechanical blending, products prepared by *in situ* or in reactor blending techniques have been proved to be superior in mechanical properties.[7] The iPP/EPR blend has attracted much attention due to its excellent toughness.[8–11]

A typical iPP/EPR is prepared *in situ* via a continuous polymerization system which includes homo-polymerization of isotactic propylene and subsequent copolymerization of propylene and ethylene in a gas-phase reactor with a Ziegler–Natta catalyst.[5,12] The products prepared by the continuous two-step copolymerization are called high impact polypropylene (hiPP) or impact polypropylene copolymer.

The excellent properties of hiPP are ascribed to its complicated composition and phase structure as a phase-separated morphology of hiPP is observed. Extensive investigations have been made to explore the composition, morphology, and phase structure of hiPP.[13–17]

It has been confirmed that hiPP is mainly formed by a matrix of isotactic polypropylene iPP in which an ethylene-propylene random copolymer EPR is finely dispersed.[10] The properties and distribution of EPR rubber in the hiPP particle (size of domains, amount of EPR, molar masses, viscosity) play a role in both reactor operation and, of course, the final product properties.[18–20]

In terms of reactor operation, one wishes to avoid the accumulation of rubber on the particle surfaces to avoid the formation of lumps or a meltdown in the fluidized bed reactor.[21] And in terms of the final product properties there may be mentioned morphological and mechanical properties.[22–25]

To date, little attention has been paid to the influence of synthesis variables on the structure and mechanical properties of iPP/EPR blend.[26,27] Kawai and Hamielec[28] have studied the effects of polymerization conditions on the particle size distribution of *in situ* iPP/EPR blends and the distribution of rubber phases in the polymer particles, but not the mechanical properties.

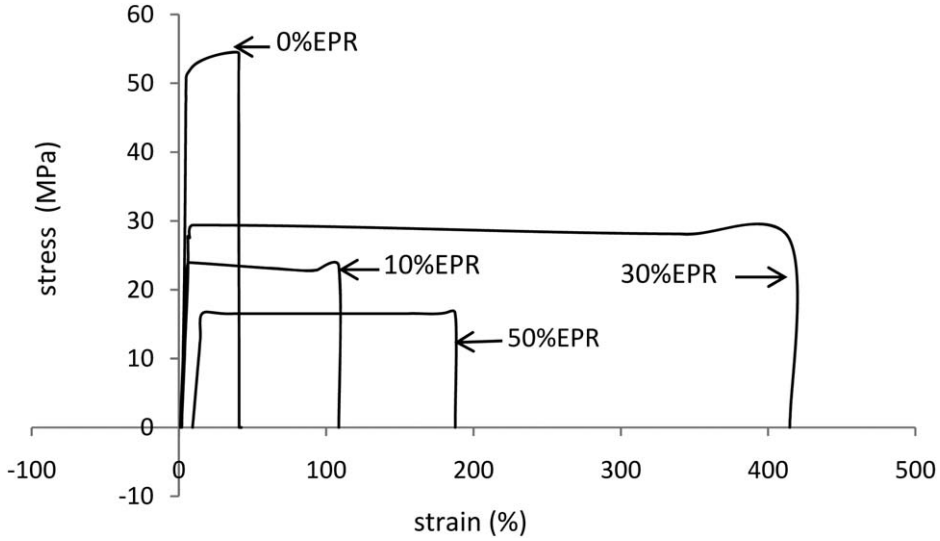

Figure 1. Stress–strain curves of hiPP samples varying the EPR content.

In recent researches, Jiniyao Chen *et al.*[29] show that the mechanical properties of the alloys are strongly influenced by the content of EPR, intrinsic viscosity ratios of EPR and the matrix and the morphology in polypropylene in reactor alloys.

In the parallel studies[30,31] when the effect of mixing ratio on the mechanical properties of polypropylene-epoxidized natural rubber (PP/ENR) blends was investigated, it was be found that the thermoplastic vulcanizates of PP/ENR at high rubber content shows an improvement in its toughness and flexibility and the elongation at break values of PP/ENR blends increases as the rubber content increases.

In another research[32] studied the mechanical and morphological properties of PP/POE blends (POE polyethylene elastomer), results shown that POE significantly improved the impact strength and breaking elongation in PP/POE blends, but resulted in a decrease of yield strength. The most useful content of POE was 15–20%.

In this article, we investigated the influence of hiPP particles morphology and operation conditions (iPP size and EPR content) on the mechanical properties of samples made from this material, by studying traction and impact tests to show the importance of the parameters mentioned previously for the mechanical properties of the final iPP/EPR product even after extrusion.

EXPERIMENTAL

Polymerization Conditions

The reactions were all carried out on a commercial $TiCl_4/MgCl_2$ Ziegler–Natta catalyst. Heptane (Sigma, France) was used as a continuous medium for the homopolymerization reactions and was treated on a molecular sieve before use.

Ethylene and propylene (Air Liquide, France) at 99.95% were used as monomers. Triethylaluminium (TEA, Witco France) was used as the co-catalyst and was diluted in heptane to obtain 1 mol/L concentration. Hydrogen with a purity of 99.95% (Air liquide, France) was used as a chain transfer agent; dicyclopentyldimethoxysilane was used as the electron donor.

Catalyst characterization: a fourth generation Ziegler–Natta catalyst was used which 80–84% of the porous volume is situated in pores smaller than 2 nm, and 89–94% of the surface area in pores of the same size, the catalyst contains 2.45% Ti, 16.8% Mg, 0.15% Al, and <0.1 Si.

The reactor used in the current study for slurry-phase and gas-phase polymerization is a 2.5 L stainless steel spherical reactor. The reactor contents are stirred with a specially designed helical agitator that passes close to the reactor wall.

The experiments were performed in a spherical high pressure reactor in a series of two steps. Step 1: Polymerization of propylene in heptane slurry at 4 bars and 70 °C, this step is variant for the runs when changing homo-polymerization times, and for 30 min when changing EPR content. Step 2: Polymerization of a 50:50 (mol) copolymer of ethylene and propylene in the gas phase at 8 bars and 40 °C (2.6 bars ethylene and 5.4 bars propylene), EPR content is 10% when changing homopolymerization time.

The crystallinity of the test strips was measured by a differential scanning calorimeter (Perkin–Elmer DSC.Pyris1). The DSC was calibrated for temperature and melting enthalpy using indium as a standard. The samples of about 10 mg weight sealed in aluminium

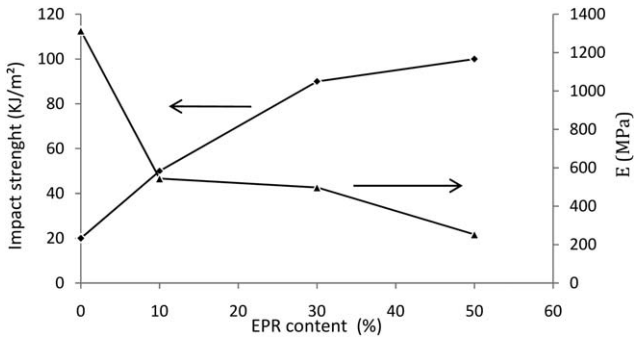

Figure 2. Young's modulus and impact strength varying the EPR content.

Table I. Mechanical and Thermal Measurements as a Function of EPR Content

Sample	EPR content (%)	E (MPa)	σ_y (MPa)	ε_y (%)	σ_b (MPa)	ε_b (%)	Impact strength (kJ/m^2)	Crystallinity X (%)
hiPP01	0	1314.5	53.36639	15.8	54.4555	40.4875	20	70.63
hiPP02	10	544.06	23.96042	6.32	23.4158	108.625	50	63.99
hiPP03	30	497.85	29.40597	9.875	27.2822	414.75	90	49.03
hiPP04	50	252.91	16.53268	15.8	16.5326	187.625	100	41.98

pans were used for the measurements. The samples were heated from 30 to 200 °C at a scanning rate of 10 °C/min under a 2 bars of nitrogen atmosphere. The crystallinity was calculated base on the theoric enthalpy of crystalline isotactic polypropylene ($\Delta H = 165$ j/g).

Morphology Analysis

Methods of Extraction. Given that EPR can be dissolved in organic solvents more easily than polypropylene, we can separate (partially or totally) the two phases to attempt to look at the influence of different factors on the final morphology. Different procedures were used to isolate the isotactic PP and amorphous material. The method used here was meant to extract as much EPR as possible from the particles while maintaining their structural integrity. The particles were placed in a Kumagawa extractor and continually washed with a stream of boiling heptane for 24–48 h. This method allowed us to extract a significant portion of the EPR (but always less than 100%), and also probably to extract the atactic fraction of the iPP matrix (estimated separately at less than 2%).

Particle Morphology. The particle morphology and domains dispersion of EPR were investigated by a scanning electron microscopy (SEM). The SEM used in this work was an HITACHI S800 with 5 nm resolution, and images were taken at a power of 10–15 kV. The polymer particle samples were covered with a fine layer of gold by vapor deposition before analysis.

Mechanical Tests

Tensile Test. The tensile test is the most mechanical test frequently used to determine the ability of a material to withstand external stresses, and which load causes a risk of rupture. This test involves subjecting a sample section to a constant stress unidirectional with a constant speed and measuring the elongation ΔL.

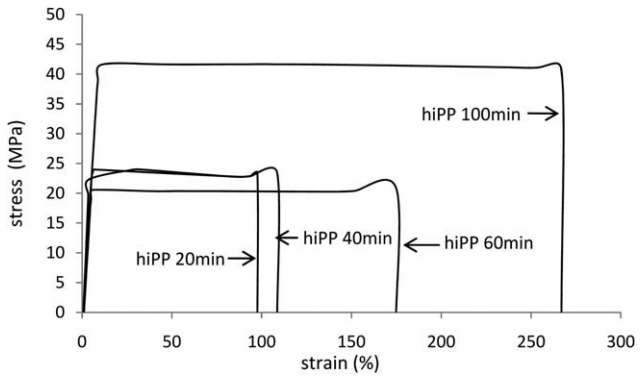

Figure 3. Stress–strain curves of hiPP samples varying the homopolymerization time.

The test strip samples were melt-pressed in a laboratory-scale injection moulding machine (BABYFAST, injection moulding machine with a piston plasticization) at 190 °C and 600 bars. Test strips were prepared as defined in the ISO standard 527-1.[33]

Stress–strain behavior in uniaxial tension was measured using a MTS traction apparatus (2/M-10kN) at room temperature, again as defined in the ISO standard 527-1. A minimum of five specimens were tested per product, and the average values were calculated for each parameter reported. The tensile strain was calculated from the ratio of the increment of the deformation length to the initial length. The tensile stress was determined by dividing the tensile load by the initial cross section. The stress–strain curves at 298 K were measured at a constant cross-head speed of 100 mm/min. Young's modulus (E) was obtained from the initial slope of the stress–strain curve. Standard deviation for tensile measurements was typically less than 10%.

Charpy Impact Test. Impact fracture energy is an important parameter characterizing toughness of materials. Impact values represent the total ability of the material to absorb impact energy. A series of Charpy impact tests were carried out for according to ISO 179.[34]

For materials tested out, the impact test consisted of fixing the notched sample horizontally on a support and then sending a known load at a certain speed, whose impact occurred at the level of the notch, and then measured the total energy at break.

The geometry of the Charpy impact test samples was rectangular with dimensions of 80 × 10 × 4 mm, conforming to the ISO 179/1eA standard. A single-edge 458 V-shaped notch (tip radius 0.25 mm, depth 2 mm) was milled in the bars with a fly-cutter using a milling machine. A series of Charpy impact tests were carried out for two temperatures according to ISO 179/1eU. For setting the test temperature, a mixture of liquid nitrogen and acetone was used. The test samples were kept in the cooling medium for at least 30 min before testing. The Charpy impact tests of the notched specimens were conducted using a Ceast Instrumented Charpy Impact Tester (Code 6545/000) at an impact speed of 2.93 m/s.

Thermal Analysis

The crystallinity (X %) of the test strips was measured by a differential scanning calorimeter (METTLER DSC) for specimens taken from the injection-moulded materials. The DSC was calibrated for temperature and melting enthalpy using indium as a standard. The samples of about 10 mg weight sealed in aluminium pans were used for the measurements. The samples were heated from 30 to 200 °C at a scanning rate of 10 °C/min under

Table II. Mechanical and Thermal Measurements as a Function of Homopolymerization Time

Sample	iPP time (min)	D_p (μm)	E (MPa)	σ_y (MPa)	ε_y (%)	σ_b (MPa)	ε_b (%)	Impact strength (kJ/m^2)	Crystallinity X (%)
hiPP05	20	480	429.36	23.96	28.4	23.41	97.62	70	64.21
hiPP02	40	688	544.06	23.96	6.32	23.41	108.62	50	63.99
hiPP06	60	717	588.64	20.55	174.88	5.69	174.88	50	63.01
hiPP07	100	750	688.20	41.60	11.07	40.65	266.94	40	65.13

a nitrogen atmosphere. The total enthalpy used to melt the sample was defined as the area under the endothermic peak for second heating, and the crystallinity was calculated on the basis of the theoretical enthalpy of crystallization of isotactic polypropylene ($\Delta H = 165$ j/g).[35]

RESULTS AND DISCUSSION

Figure 1 shows the stress-strain curves of hiPP as a function of rubber content. As can be observed the addition of EPR changed the stress–strain curve considerably. The iPP/EPR blends containing a higher proportion of EPR have distinct elastic and plastic regions. The iPP presents almost no plastic behavior while the hiPP with 10%, 30%, and 50% in EPR, who present very large values of deformation. This suggests that the presence of rubber EPR (amorphous phase) increases the ability of the material to be deformed (plastic step).[36] The more the product undergoes a long plastic deformation before breaking, the more the product is considered ductile. The tensile strength (break) of the blend iPP/EPR is higher than that of pure iPP.[35] At high rubber content degrees (>30), the tendency is inversed and the material loses some of its ductility, 414.75% and 187.62% for 30% and 50% of EPR respectively, either lowering of 45% of the ductility of the material. This can be explained by the fact that when EPR reaches or exceeds a certain threshold the material became less ductile. The presence in excess of the amorphous phase (EPR) superior to 30% reduces the material's ability to be deformed without breaking.

Figure 2 shows the variation of the young modulus and impact strength versus rubber content. As seen in this Figure, for each sample, the elastic modulus decreases with a decrease in EPR amount.[37,38] Also increasing rubber content has a significant effect on impact strength properties. The impact strength begins to evolve as soon as the content of the rubber increases.[39,40] Adding rubber particles in the iPP matrix reduces the elastic modulus from 1314.5 to 252.91 MPa and the impact strength increases from 20 to 100 kJ/m^2 for 0% and 50% of EPR, respectively.

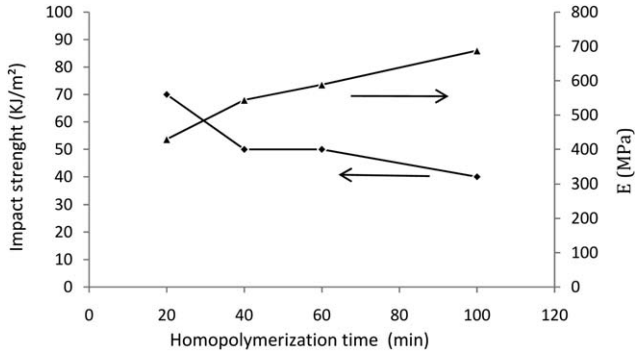

Figure 4. Young's modulus and notched impact strength varying the homopolymerization time.

These results can be explained morphologically by the discontinuous distribution of rubber domains in the iPP matrix at low EPR content. However, these domains tend to form a more continuous network as the EPR content increases. Thus, the iPP bears the physical load, and the EPR simply helps to disperse the mechanical energy and acts as a concentrator of constraints, the latter are directly related to the content of the EPR.[41]

The advanced impact toughness of the hiPP blends can be interpreted as a consequence of their high EPR content and the good compatibility between the different components in the multiphase system.[29] The loss of strength is related to the elastic amount of the rubber material. The greater the amount of EPR is, the more elastic and the less hard product tend to be. From a chemical view point, these observations reveal that the more hiPP is crystalline, the more Young's modulus E is high. The crystallinity of hiPP decreases with the increase in the proportion of EPR as shown in Table I.[42]

The relationship between elastic modulus and strength impact, as shown in Figure 2, is due to the nature of the rubber phase which results in the dispersion of the mechanical energy of the shock in the hiPP particle; thus iPP can support the physical load.

The influence of particle size of iPP occurred during the homopolymerization by changing homopolymerization reaction time on morphology and mechanical properties of the material are reported. Results show that when the particle size is small, the material has a more significant impact resistance.

Figure 3 and Table II show that the sample hiPP07 (100 min) has a ductile behavior with a modulus of elasticity of 688.20 MPa and an elongation at break of the order of 266.94%. Whereas hiPP05 (20 min) has a much lower value for the modulus of elasticity (429.36 MPa) and a very low value for elongation at break (97.62%). Increasing the duration of homopolymerization increases the modulus of elasticity which makes a more rigid final product. The mechanical tensile strength is similar for the products which have homo-polymerization time less or equal to 60 min, and a much great value in the case of 100 min is observed.

The impact test is designed to measure the resistance of a material to the break. In Figure 4, it can be seen that notched impact

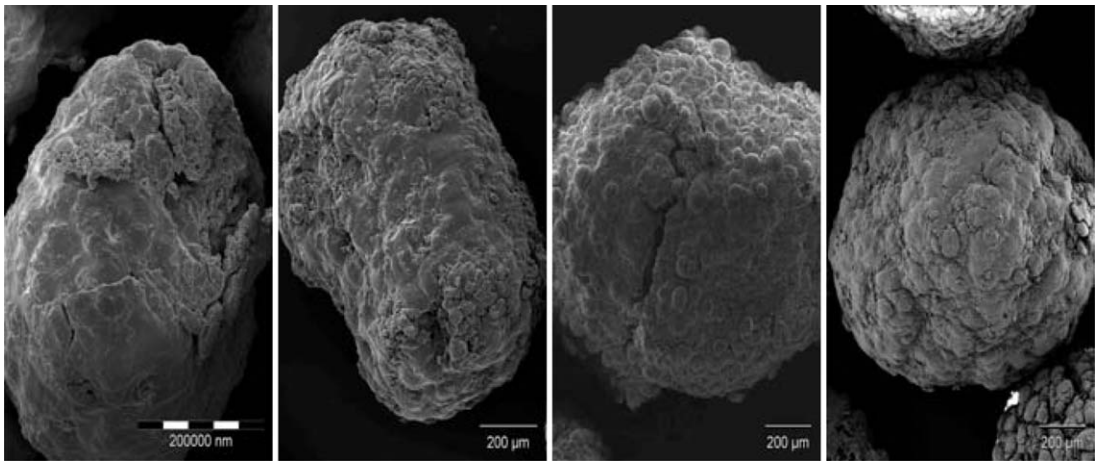

Figure 5. SEM images of hiPP particles produced with 20, 40, 60, and 100 min as time of homopolymerization. Clockwise from the left.

strength decreases with the size of the iPP particle. It decreased from 70 to 40 kJ m^{-2} in an interval of 20 to 100 min. This change can be explained by the distribution of the elastomer in the small iPP particle. The larger iPP particle is the more the EPR domains are remote from each other, there is no connection between the rubber fields; thus, the material is less impact resistant. It is postulated that the iPP size and connectivity of the rubber domains EPR play an important role in the final mechanical properties of hiPP.

Figure 5 shows four SEM images of hiPP particles, the changes are obvious concerning the rubber pooling in the surface of the particle. In the image of the left, representative of the smaller iPP particles (20 min), EPR pooling that covers a large part of the surface is often visible.[28] After 40 min, the same phenomenon is observed to a lesser degree. However, after 60 and 100 min, examination of the micrographs revealed that the pooling seems to have disappeared from the surface. The homopolymerization time and thus iPP particle size alter the morphology and mechanical properties of the hiPP. According to images of SEM in Figure 5, the longer the time of the first polymerization step is, the larger the iPP particle tends to be and the least the rubber settles on the surface of the hiPP[26]; therefore, the final material is less resistant to impact. In fact, EPR tends to form a continuous network on particle surface after extrusion and helps to disperse the mechanical energy.

CONCLUSIONS

Investigations on the mechanical properties that can provide morphological changes on hiPP particles have helped us to identify the influence of some synthesis variables of the hiPP on the strength of materials and mechanical performance. These experiments have allowed us to show, as expected, that the influence of the addition of rubber to the iPP crystalline matrix improves its resistance. The EPR content has an important role on the mechanical properties[29] and the deformation of the final product. Increasing the EPR content in hiPP is an approach for improving the toughness of product. The iPP/EPR *in situ* blends show excellent mechanical properties with a good balance between toughness and rigidity. But, at high rubber content (>30) the tendency is inversed and the material loses some of its ductility. Conversely, the highest level of mechanical resistance is obtained with the smallest iPP particles by reducing the interparticle distance and increasing the energy absorption capacity.

REFERENCES

1. Bhaskar, H. B.; Sharief, A. *J. Mech. Eng. Sci.* **2012**, *3*, 281.
2. Jeefferie, A. R.; Mohamad, N.; Ab Maulod, H. E. *J. Elastomers Plast.* **2012**, *45*, 239.
3. Pang, Y.; Dong, X.; Zhang, X.; Liu, K.; Chen, E.; Han, C.; Wang, C. D. *Polymer* **2008**, *49*, 2568.
4. Zhao, S.; Cai, Z.; Xin, Z. *Polymer* **2008**, *49*, 2745.
5. Fan, Z. Q.; Zhang, Y. Q.; Xu, J. T.; Wang, H. T.; Feng, L. X. *Polymer* **2001**, *42*, 5559.
6. Pasquini, N., Ed. In Polypropylene Handbook; Hanser Publishers: Munich, **2005**.
7. Nitta, K.; Kawada, T.; Yamahiro, M.; Mori, H.; Terano, M. *Polymer* **2000**, *41*, 6765.
8. Debling, J. A.; Zacca, J. J.; Ray, W. H. *Chem. Eng. Sci.* **1997**, *52*, 1969.
9. Hermanová, S.; Tochácek, J.; Jancár, J.; Kalfus, J. *Polym. Degrad. Stab.* **2009**, *94*, 1722.
10. Mirabella, J. F. M. *Polymer* **1993**, *34*, 1729.
11. Wang, L. X.; Huang, B. T. J. *Polym. Sci. Polym. Phys.* **1990**, *28*, 937.
12. Debling, J. A.; Ray, W. H. *J. Appl. Polym. Sci.* **2001**, *81*, 3085.
13. Chen, R.; Shangguan, Y.; Zhang, C.; Chen, F.; Harkin-Jones, E.; Zheng, Q. *Polymer* **2011**, *52*, 2956.
14. Chen, Y.; Chen, Y.; Chen, W.; Yang, D. C. *J. Appl. Polym. Sci* **2008**, *108*, 2379.
15. Song, S. J.; Wu, P. Y.; Feng, J. C.; Ye, M. X.; Yang, Y. L. *Polymer* **2009**, *50*, 286.
16. Zhang, C. H.; Shangguan, Y. G.; Chen, R. F.; Wu, Y. Z.; Chen, F.; Zheng, Q.; Hu, G. H. *Polymer* **2010**, *51*, 4969.

17. Zhang, C. H.; Shangguan, Y. G.; Chen, R. F.; Zheng, Q. *J. Appl. Polym. Sci.* **2011**, *119*, 1560.
18. Tanem, B. S.; Kamfjord, T.; Augestad, M.; Løvgren, T. B.; Lundquist, M. *Polymer* **2003**, *44*, 4283.
19. Marcus, K.; Sole, B.; Patil, R. *Macromol. Symp.* **2002**, *178*, 39.
20. Ibhadon, A. O. *J. Appl. Polym. Sci.* **1999**, *71*, 579.
21. Xu, J.; Feng, L.; Yang, S.; Wu, Y.; Yang, Y.; Kong, X. *Polymer* **1997**, *38*, 4381.
22. Bucknall, C. B. *Makromol. Chem. Macromol. Symp.* **1990**, *38*, 1.
23. Fond, C.; Lobbrecht, A.; Schirrer, R. *Int. J. Fracture* **1996**, *77*, 141.
24. Van Der Wal, A.; Verheul, A. J. J.; Gaymans, R. J. *Polymer* **1999**, *40*, 6057.
25. Jang, B. Z.; Uhlmann, D. R.; Vander, S. J. B. *Polym. Eng. Sci.* **1985**, *25*, 643.
26. Jiang, T.; Chen, H.; Ning, Y.; Kuang, D.; Qu, G. *J. Appl. Polym. Sci.* **2006**, *101*, 1386.
27. Chen, Y.; Chen, Y.; Chen, W.; Yang, D. *Eur. Polym. J.* **2007**, *43*, 2999.
28. Kawai, H.; Hamielec, A. *Polym. React. Eng.* **1999**, *7*, 501.
29. Jinyao, C.; Jian, K.; Junqi, Y.; Shipeng, Z.; Feng, Y.; Ya, C.; Ming, X.; Huilin, L. *J. Polym. Res.* **2015**, *22*, 180.
30. Mohamad, N.; Zainol, N. S.; Rahim, F. F.; Ab Maulod, H. E.; Abd Rahim, T.; Shamsuri, S. R.; Azam, M. A.; Yaakub, M. Y.; Bin Abdollah, M. F.; Abd Manaf, M. E. *Proc. Eng.* **2013**, *68*, 439.
31. Mohamad, N.; Nur Sharafina, Z.; Ab Maulod, H. E.; Yuhazri, M. Y.; Jeefferie, A. R. *Int. J. Automot. Mech. Eng.* **2013**, *8*, 1305.
32. Liu, G. Y.; Qiu, G. X. *Polym. Bull.* **2013**, *70*, 849.
33. Plastics-Determination of Tensile Properties, ISO 527, **1993**.
34. Plastics-Determination of Charpy Impact Properties-Part1: Non Instrumented Impact Test, ISO 179-1, **2010**.
35. Brandrup, J.; Grulke, E. A.; Immergut, E. H., Eds. In Polymer Handbook; Wiley: Canada, **1989**.
36. Treloar, L. R. G. In The Physics of Rubber Elasticity, 3rd ed.; Clarendon Press: Oxford, **1975**.
37. Pukanszky, B.; Tudos, F.; Kallo, A.; Bodor, G. *Polymer* **1989**, *30*, 1407.
38. Gupta, A. K.; Purwar, S. N. *J. Appl. Polym. Sci.* **1984**, *29*, 3513.
39. Starke, J. U.; Michler, G. H.; Grellmann, W.; Seidler, S.; Gahleitner, M.; Fiebig, J.; Nezbedova, E. *Polymer* **1998**, *39*, 75.
40. Kotter, I.; Grellmann, W.; Koch, T.; Seidler, S. *J. Appl. Polym. Sci.* **2006**, *100*, 3364.
41. Bucknall, C. B. *Adv. Polym. Sci.* **1978**, *27*, 121.
42. Karger-Kocsis, J.; Csikai, I. *Polym. Eng. Sci.* **1987**, *27*, 241.